

## APPLICATIONS OF A VENUS THERMOSPHERIC CIRCULATION MODEL

S. W. Bougher, R. E. Dickinson, E. C. Ridley, and R. G. Roble  
National Center for Atmospheric Research  
Boulder, CO 80307

A variety of Pioneer Venus observations suggest a global scale, day-to-night Venus thermospheric circulation. The two-dimensional hydrodynamic model of Dickinson and Ridley (1977) correctly predicted the gross characteristics of this largely symmetric circulation. However, it failed to calculate the observed cold nightside temperatures, and the exact phases and densities of the neutral constituents. This paper presents model studies of the dynamics and energetics of the Venus thermosphere, in order to address new driving, mixing and cooling mechanisms for an improved model simulation.

The adopted approach has been to re-examine the circulation by first using the previous two-dimensional code to quantify those physical processes which can be inferred from the Pioneer Venus observations. Specifically, the model was used to perform sensitivity studies to determine the degree to which eddy cooling, eddy or wave drag, eddy diffusion and  $15\text{ }\mu\text{m}$  radiational cooling are necessary to bring the model temperature and composition fields into agreement with observations. Three EUV heating cases were isolated for study.

Global temperature and composition fields in good agreement with Pioneer data were obtained. Large scale horizontal winds  $\leq 220\text{ m/s}$  were found to be consistent with the observed cold nightside temperatures and dayside bulges of O, CO and  $\text{CO}_2$ . Fine tuning required that an eddy coefficient  $\leq 20\%$  of previous one-dimensional models be used for nightside diffusion ( $K = 7.5 \times 10^6\text{ cm}^2/\text{s}$ ). Very little eddy diffusion was required for the dayside ( $K \leq 4 \times 10^6\text{ cm}^2/\text{s}$ ). Observed dayside temperatures were obtained by using a 7-19% EUV heating efficiency profile. The enhanced  $15\text{ }\mu\text{m}$  cooling needed for thermal balance is obtained using the best rate coefficient ( $K_{\text{CO}_2-\text{O}} = 5 \times 10^{-13}\text{ cm}^3/\text{s}$ ) available for atomic O collisional excitation of  $\text{CO}_2(0, 1, 0)$ . Eddy conduction was not found to be a viable cooling mechanism due to the weakened global circulation. The strong  $15\text{ }\mu\text{m}$  damping and low EUV efficiency imply a very weak dependence of the general circulation to solar cycle variability. Finally, the NCAR terrestrial thermospheric general circulation model (TGCM) was adapted for Venus inputs using the above two-dimensional model parameters, to give a three-dimensional benchmark for future Venus modelling work.

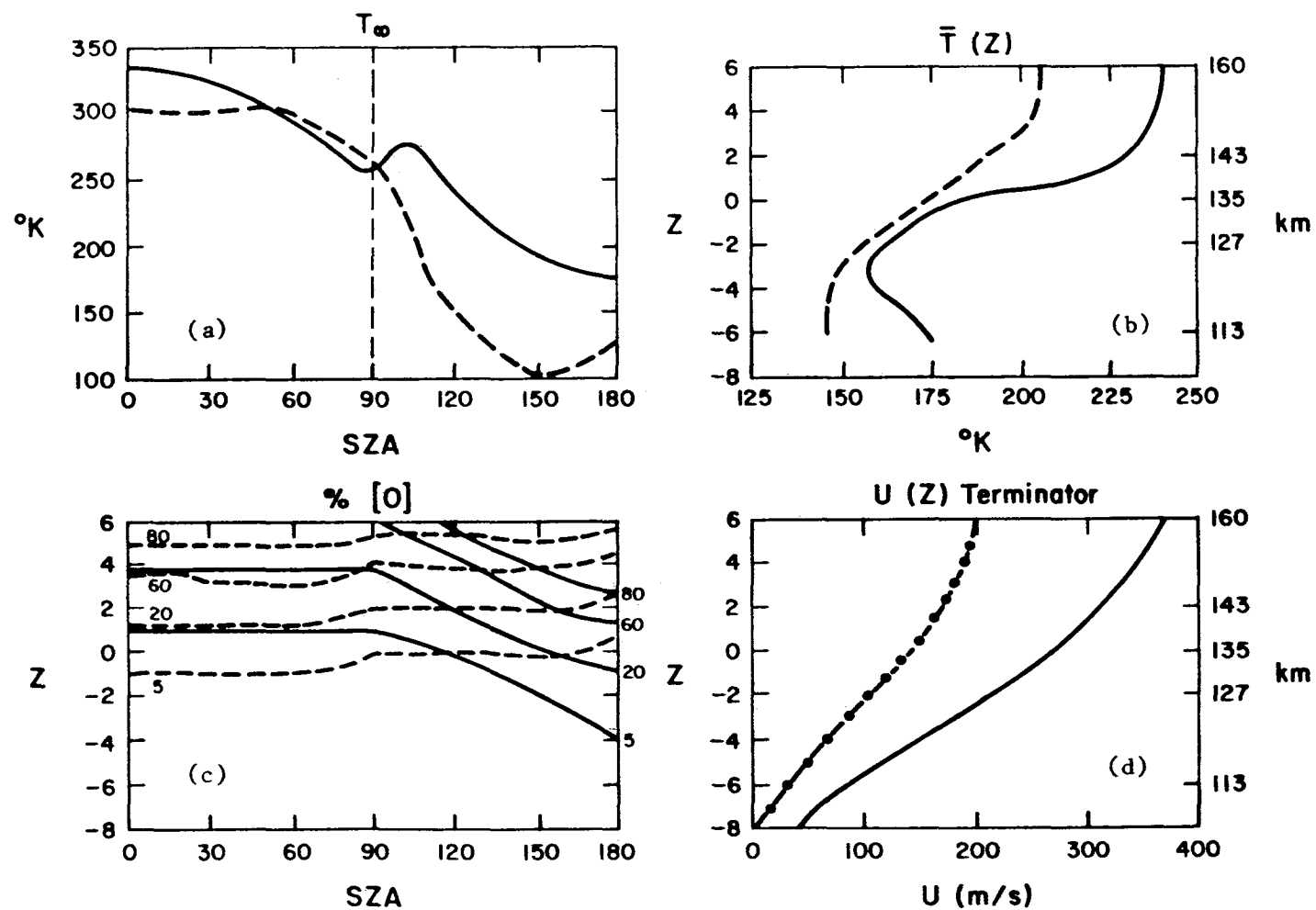


Figure 1. Comparisons of Dickinson and Ridley (1977) (DRM2) predictions and Pioneer Venus (PV) observations (\_\_\_\_\_DRM2; ----PV; -.-. Mayr et al., 1980) where  $z = \log(5 \times 10^{-3} \mu\text{bar/p})$ .

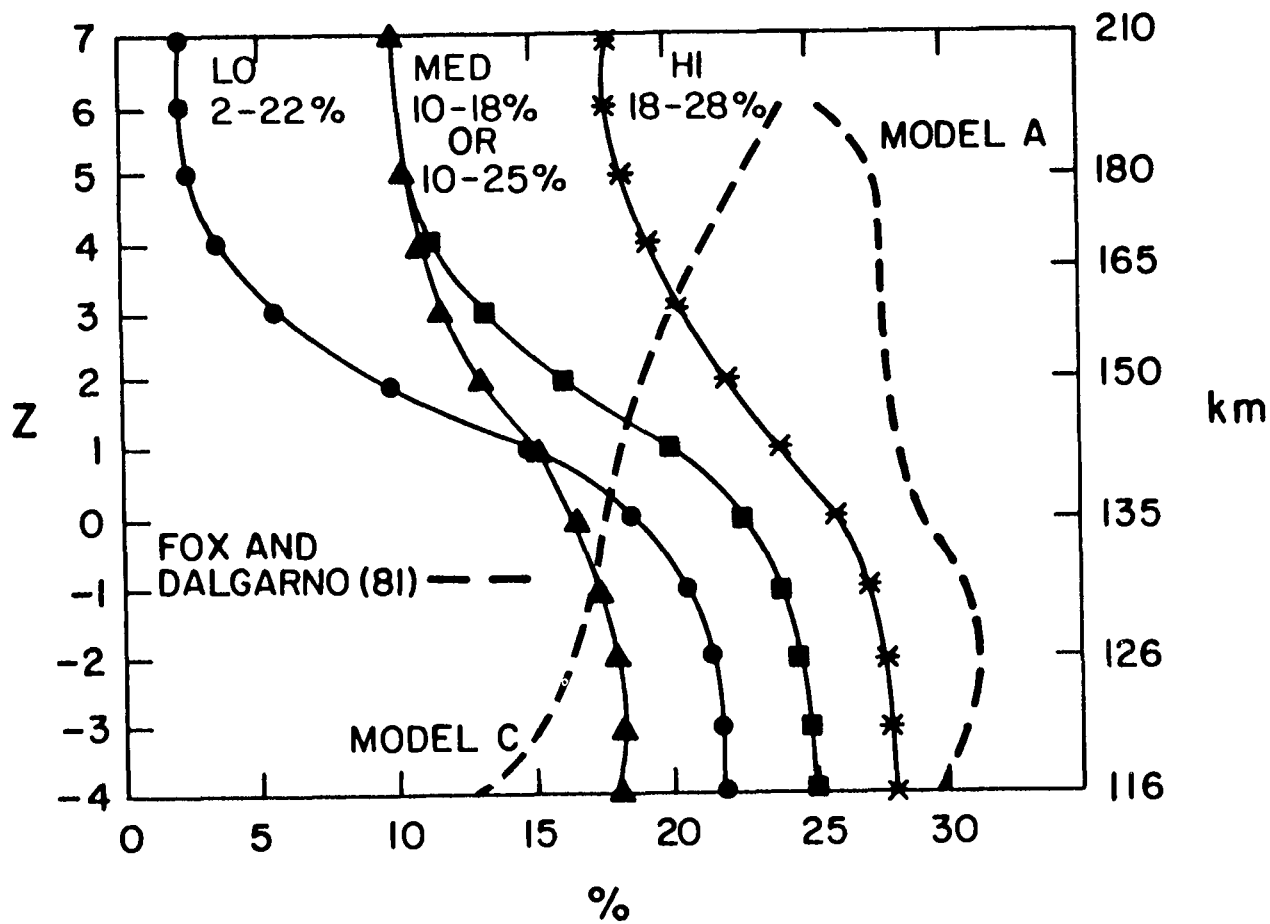


Figure 2. EUV heating efficiency profiles.

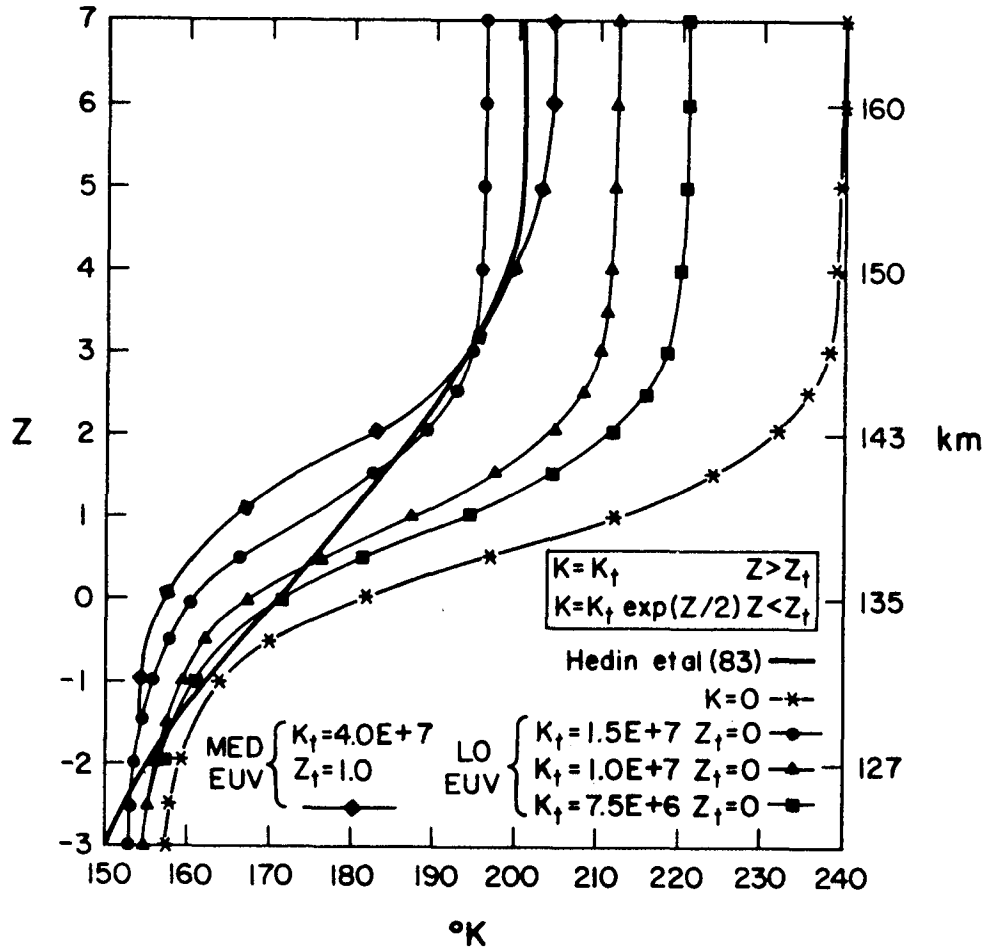


Figure 3. Global mean Venus one-dimensional thermospheric temperature profiles: eddy cooling tests. Here  $K_t$  is the turbopause value of the eddy coefficient and  $Z_t$  corresponds to the turbopause level.

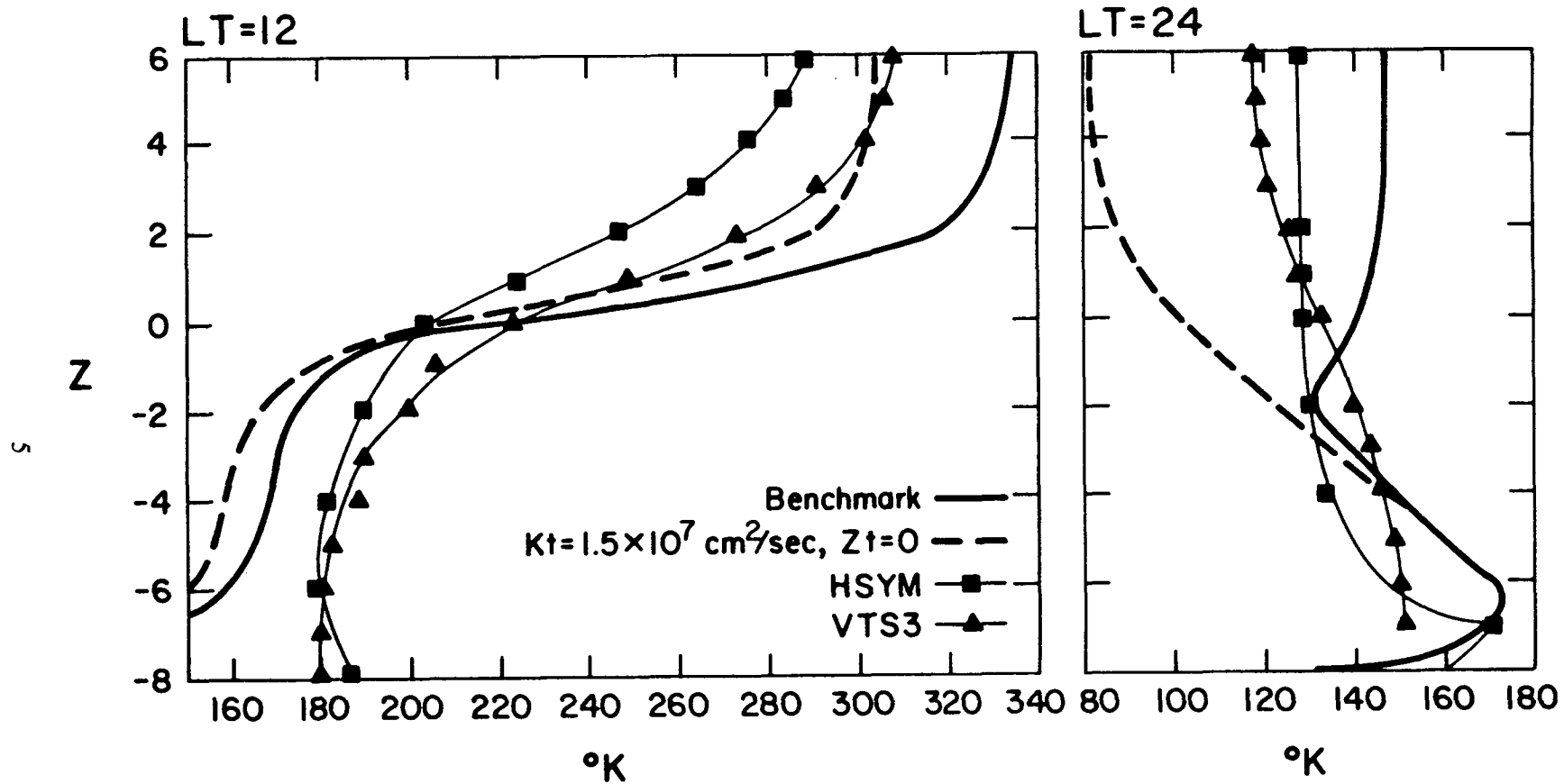


Figure 4. Venus two-dimensional model temperature response to eddy cooling. HSYM corresponds to the Keating et al. (1984) model atmosphere, and VTS3 to the Hedin et al. (1983) empirical model.

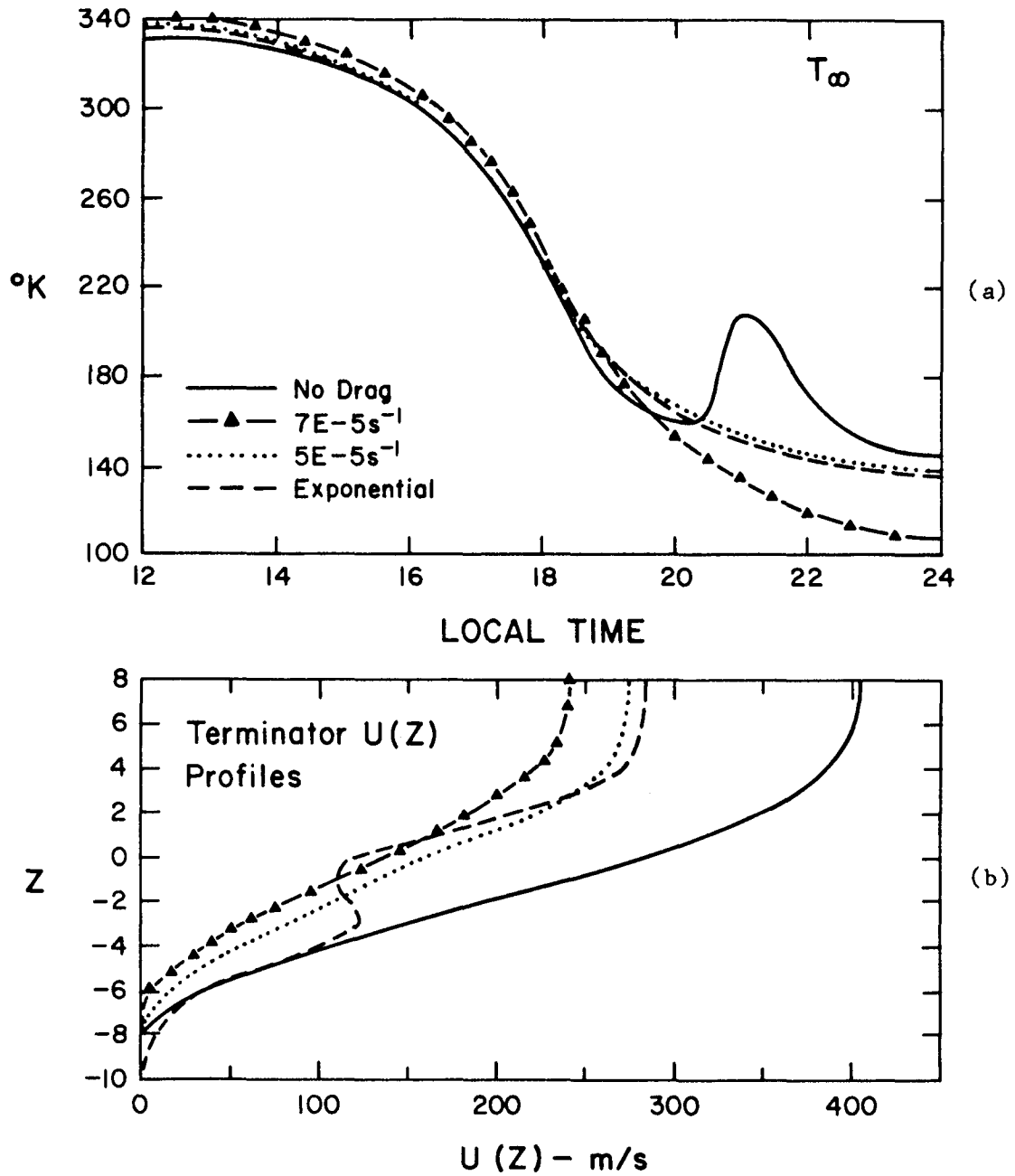


Figure 5. Venus two-dimensional model response to viscous drag tests. The effects are shown for various adjustments of a Rayleigh friction coefficient ( $K_{\text{RA}}$ ) (a)  $T_{\infty}$ , (b) terminator  $u(z)$  profiles.

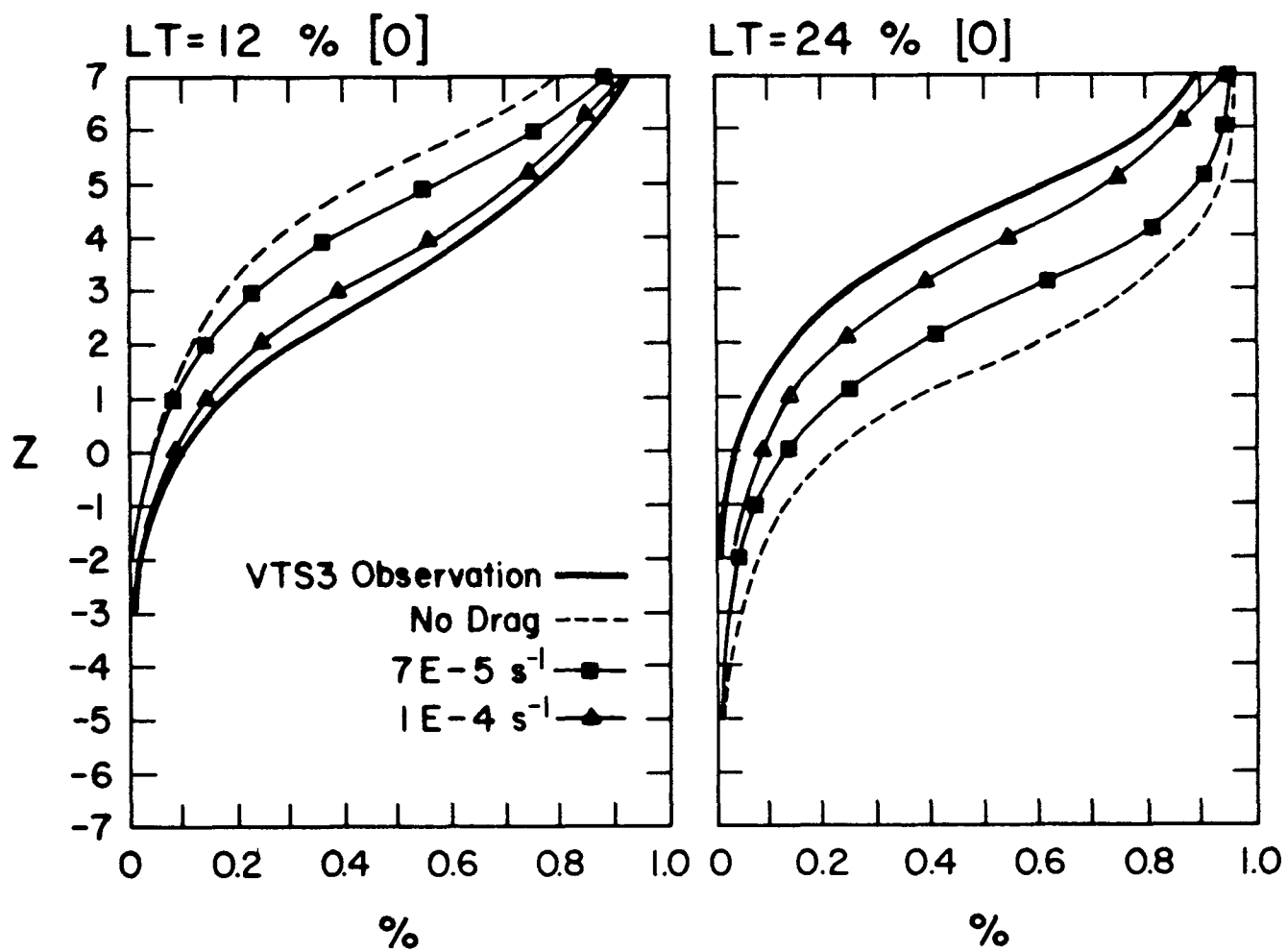


Figure 6. Venus two-dimensional model response to viscous drag tests (c) composition.

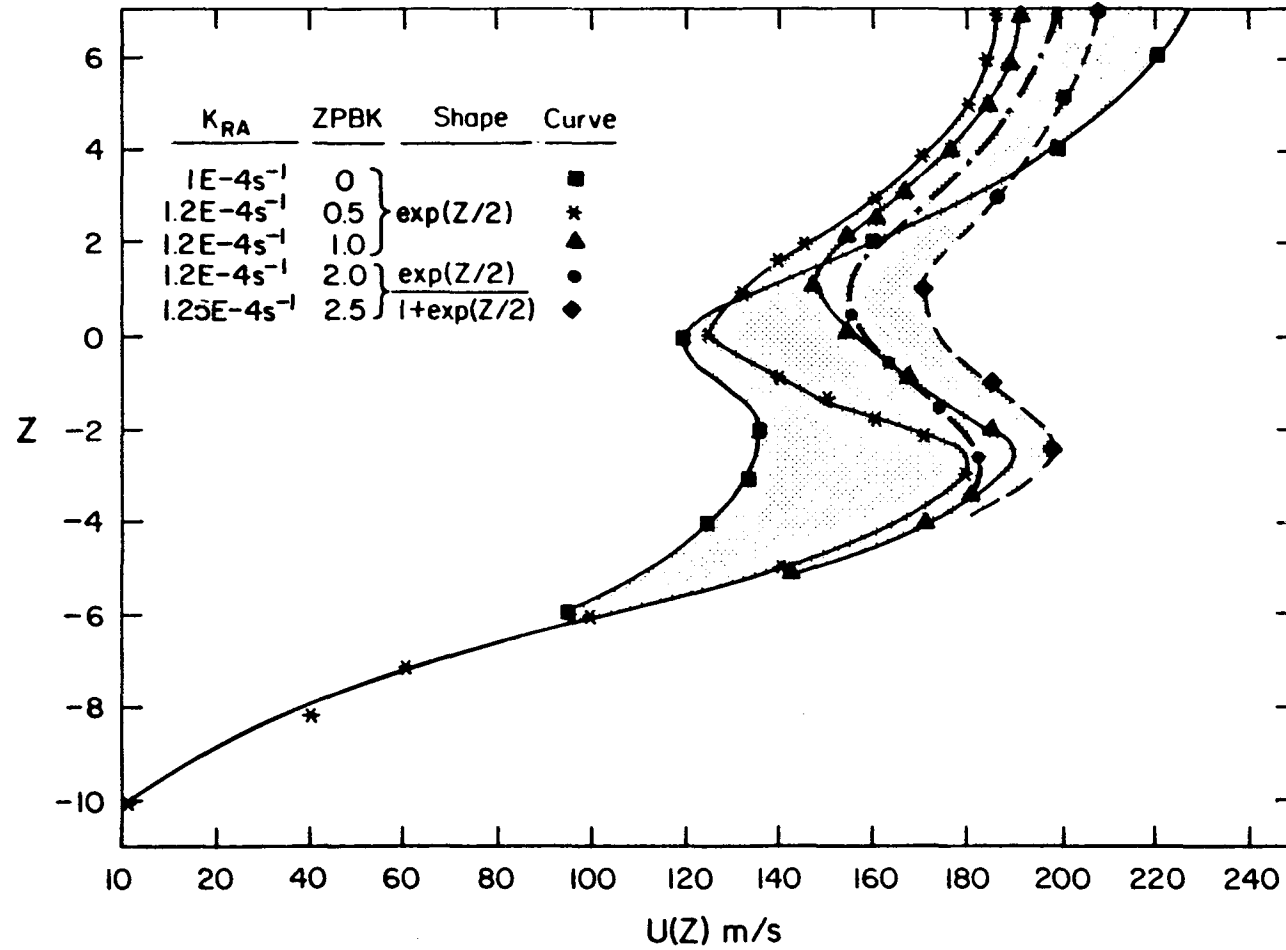


Figure 7. Family of terminator horizontal wind profiles. Various drag profile shapes and  $K_{RA}$  magnitudes were examined to obtain the best day-night distribution of model composition and temperature fields.



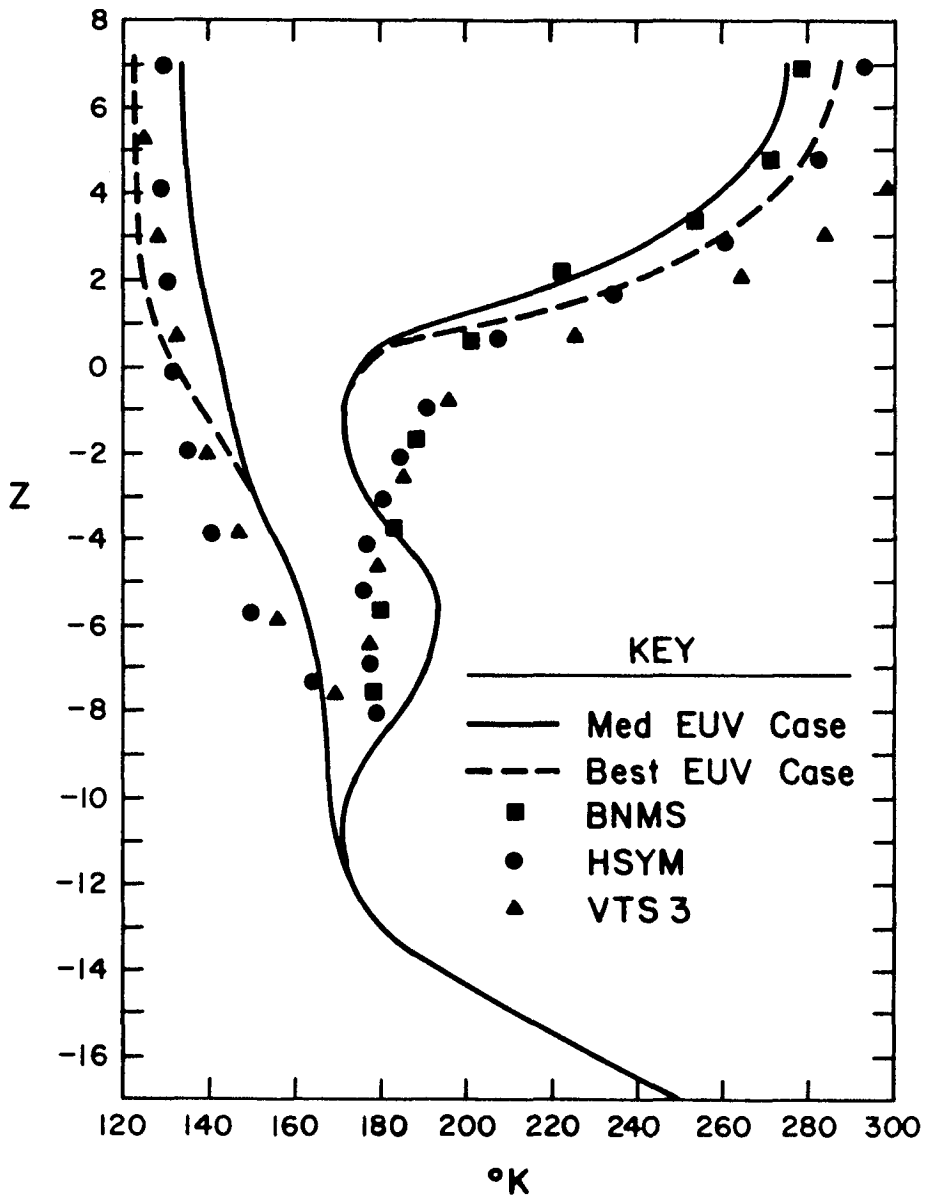


Figure 8. One-dimensional radiative transfer model reference temperatures: dayside and nightside mean profiles. These were calculated using the enhanced  $15\text{ }\mu\text{m}$  cooling ( $K_{\text{CO}_2-\text{O}} = 5 \times 10^{-13} \text{ cm}^3/\text{s}$ ) possible via atomic O collisional excitation of  $\text{CO}_2(0, 1, 0)$ . Results are given for the BEST EUV case (7-19% profile) heating.

Best Parameter Adjustments for Each EUV Efficiency Case

Parameter	Low (2-22%)	Medium (10-25%)	High (18-28%)	Best (7-19%)
<u>Eddy Cooling</u>				
DY: $K_{\max}/ZPBK$	$1.0 \times 10^7 / 0$ (NG)	$4 \times 10^7 / 0$ (NG)	-	none
<u>15 <math>\mu</math>m Cooling</u>				
$k(CO_2-O)$	$2 \times 10^{-13}$	$7.5 \times 10^{-13}$	$1.75 \times 10^{-12}$	$5 \times 10^{-13}$
<u>Eddy Drag</u>				
$K_{RA}$	$1-1.25 \times 10^{-4} s^{-1}$	$1-1.2 \times 10^{-4} s^{-1}$	-	$1.2 \times 10^{-4} s^{-1}$
ZPBK	0	0+1	-	2.0
<u>Eddy Diffusion</u>				
DY: $K_{\max}/ZPBK$	$< 5 \times 10^6 / 0$	none	-	none
NT: $K_{\max}/ZPBK$	$1-1.5 \times 10^7 / 0$	$7 \times 10^6 / 0$	-	$7.5 \times 10^6 / \phi$
<u>SZAF</u>	2.0	$\geq 2.0$	-	$\geq 2.0$
<u>Efficiency</u>				
<u>Profile Shape</u>				
$\epsilon(z)$	$0.02+0.4*f(p)$	$0.10+0.3*f(p)$	$0.18+0.2*f(p)$	$0.07+0.24*f(p)$
$f(p)$	$0.5 / (1. + \frac{1.05 \times 10^{-3}}{p})$	$0.5 / (1. + \frac{1.05 \times 10^{-3}}{p})$	$0.5 / (1. + \frac{1.05 \times 10^{-3}}{p})$	$0.5 / (1. + \frac{4.73 \times 10^{-4}}{p} (\frac{T}{200})^{0.55})$
$\epsilon_{Top}$	2%	10%	18%	7%
$\epsilon_{Bot}$	22%	25%	28%	19%

Figure 9. Best parameter adjustments for each EUV efficiency case. The 7-19% case was isolated for further study since the 15 $\mu$ m cooling  $K_{CO_2-O}$  rate adopted is comparable to that inferred by Sharma and Nadile (1981) from a terrestrial rocket measurement of  $CO_2$  emission limb radiance above 100 km.

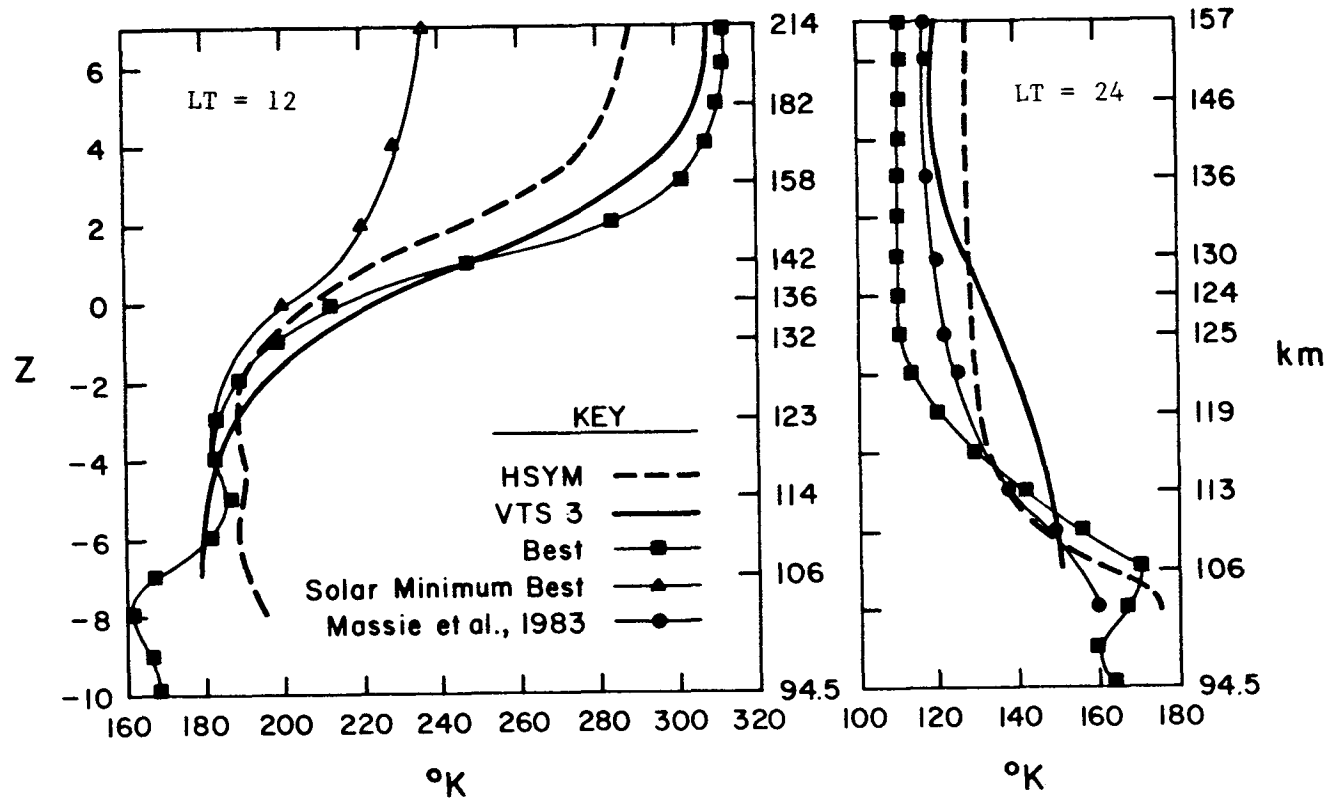


Figure 10. Venus two-dimensional model temperature: BEST EUV case. Comparisons are made with Pioneer Venus model atmospheres (HSYM and VTS3) as well as with the adopted nightside temperature profile of Massie et al. (1983). Solar minimum fluxes of Heroux and Hinteregger (1978) ( $F_{10.7} = 80 \times 10^{-22} \text{ Wm}^{-2} \text{ Hz}^{-1}$ ) are used to derive a new noon temperature profile. Exospheric temperatures are seen to vary by nearly  $70^\circ\text{K}$  from solar minimum to solar maximum conditions.

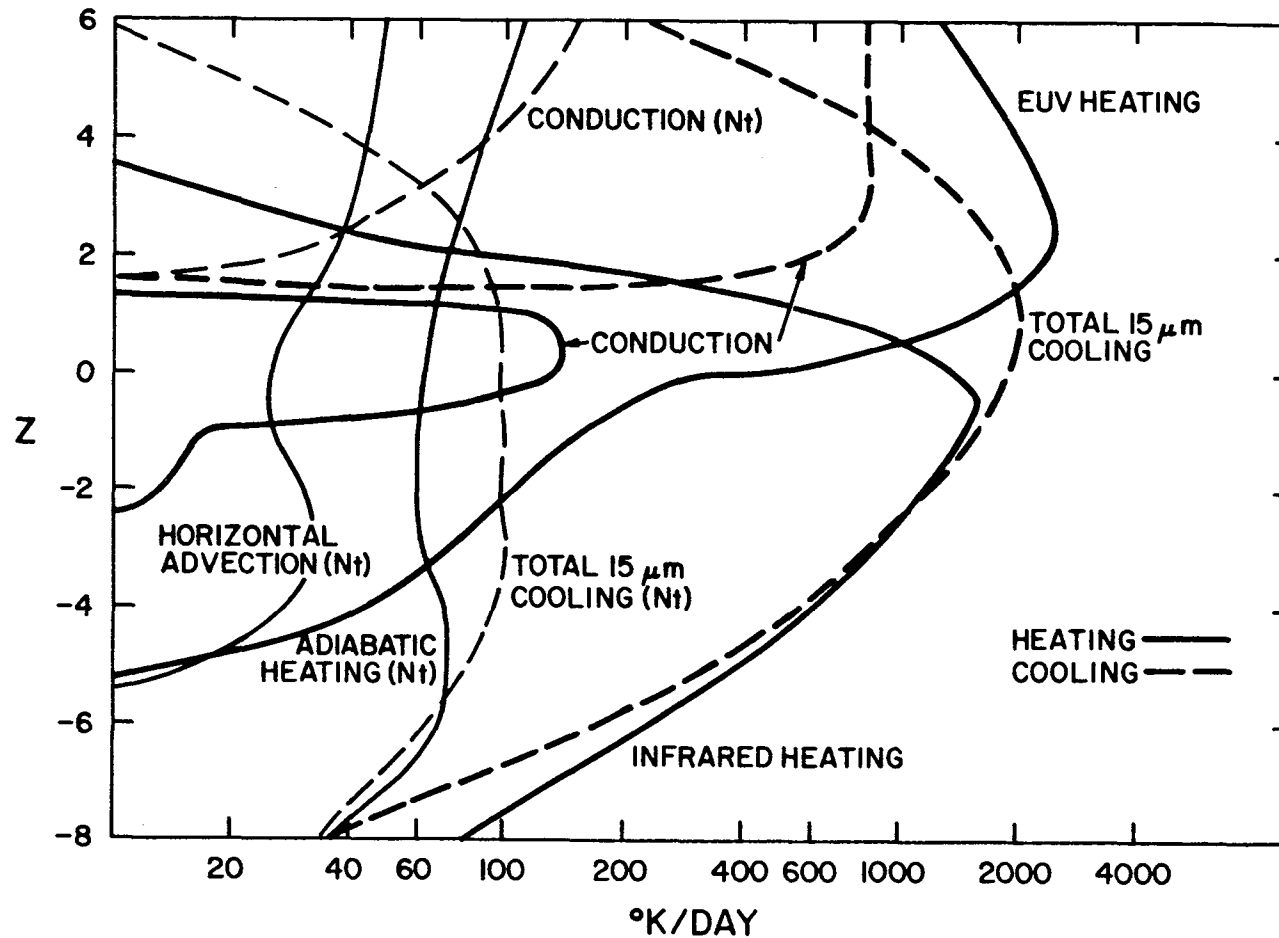


Figure 11. Heating and cooling rates at 60° and 120° SZA: BEST EUV case. Weakened adiabatic heating and horizontal advection on the nightside (plus improved 15  $\mu\text{m}$  cooling) combine to give cooler nightside temperatures than Dickinson and Ridley (1977).

# Model and Empirical Data Set Comparisons at 150 km

<u>Averages Over Dayside (LT = 12-16 hr)</u>						
	Hedin et al. (1983)		Keating et al. (1984)			2-D Model
	H	H/2D	K	K/2D	H/K	6/84
$n_T$	1.39(10)	1.01	1.36(10)	0.99	1.02	1.38(10)
$n_O$	4.70(9)	1.74	3.56(9)	1.32	1.32	2.70(9)
$n_{CO}$	2.32(9)	1.05	1.80(9)	0.82	1.29	2.20(9)
$n_{CO_2}$	5.82(9)	0.77	7.13(9)	0.95	0.82	7.52(9)
$n_{N_2}$	1.01(9)	1.11	1.04(9)	1.15	0.97	9.06(8)
$n_{He}$	6.39(6)	1.73	4.57(6)	1.24	1.40	3.70(6)
T	271.3	0.97	252.5	0.90	1.07	280
<u>Averages Over Nightside (LT = 19-24 hr)</u>						
$n_T$	1.43(9)	1.15	1.39(9)	1.12	1.03	1.24(9)
$n_O$	1.12(9)	1.14	1.03(9)	1.05	1.09	9.80(8)
$n_{CO}$	1.10(8)	1.26	1.09(8)	1.25	1.01	8.73(7)
$n_{CO_2}$	9.70(7)	0.89	9.90(7)	0.91	0.98	1.09(8)
$n_{N_2}$	7.63(7)	1.17	9.74(7)	1.50	0.78	6.51(7)
$n_{He}$	1.49(7)	0.14	3.11(7)	0.29	0.48	1.08(8)
T	119.3	0.98	129.8	1.06	0.92	122.1

Figure 12. Model and empirical data set comparisons at 150 km.

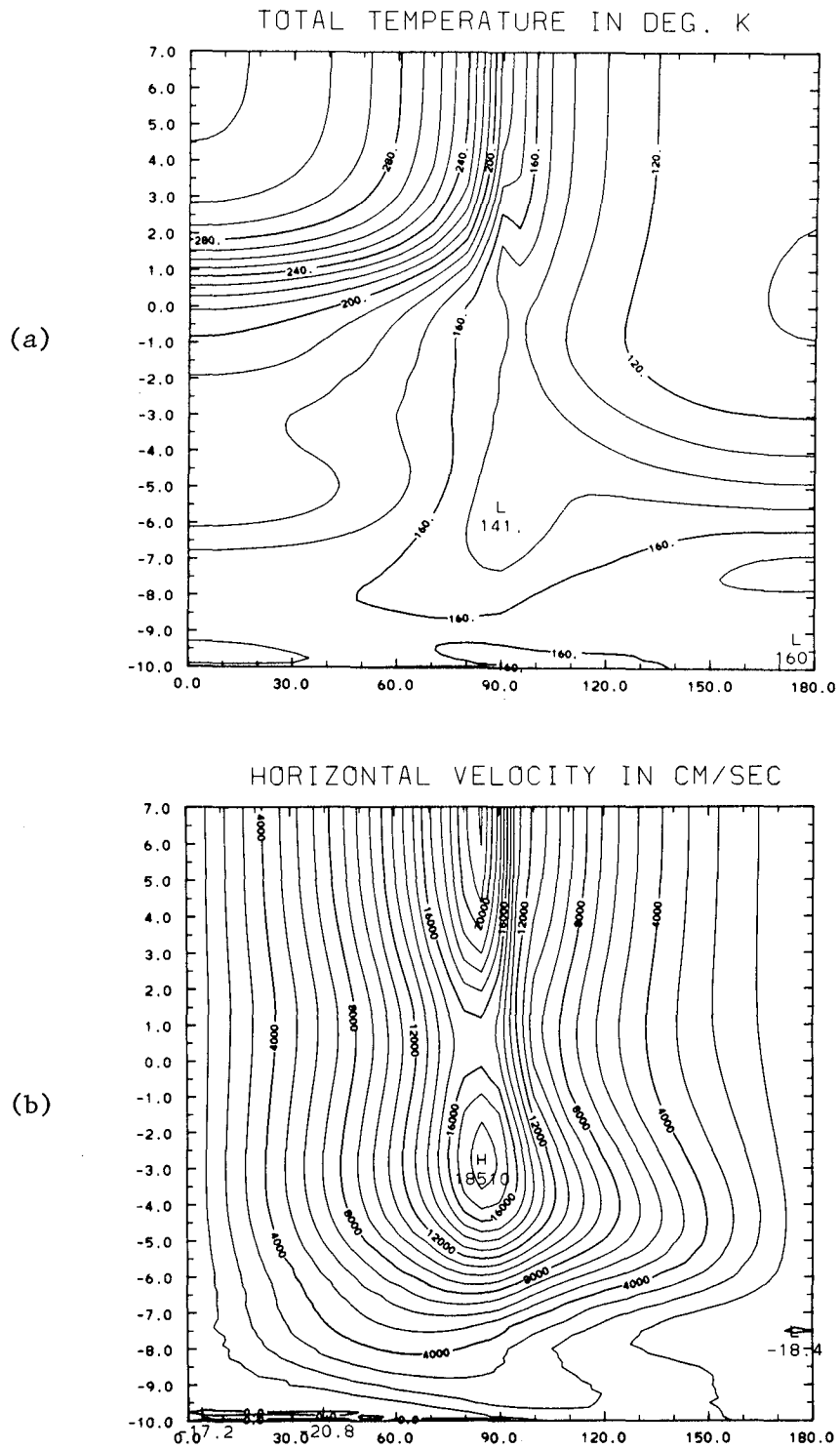


Figure 13. Best EUV case contour plots (SZA vs Z):  
 (a) Total temperature in deg K.  
 (b) Horizontal velocity in cm/sec.

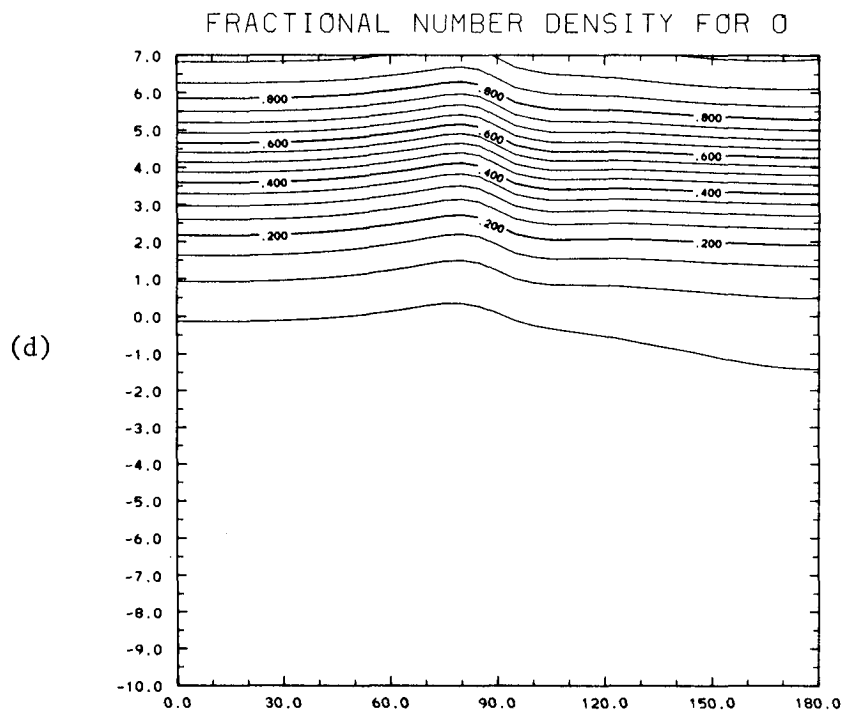
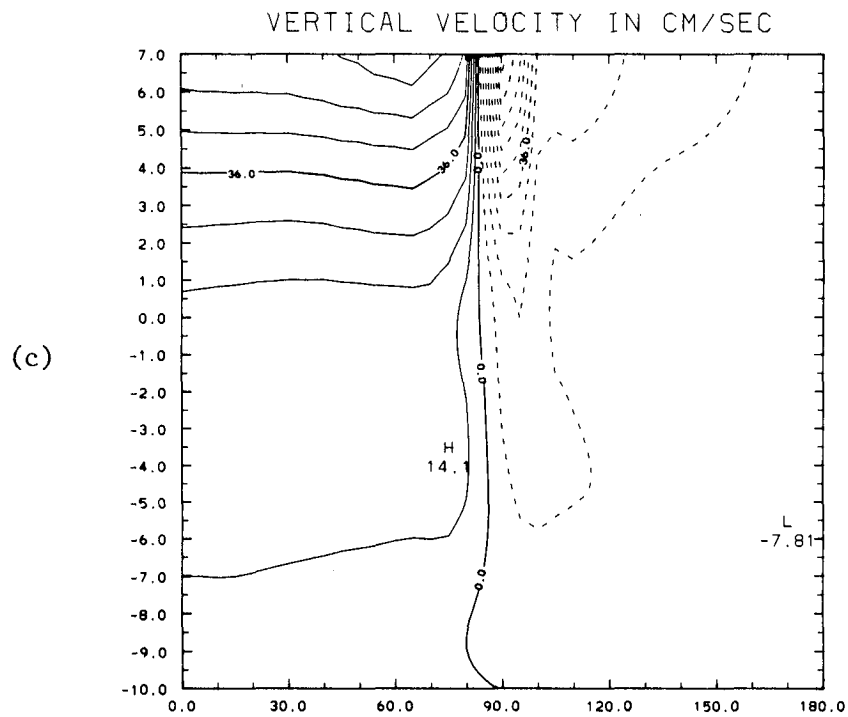


Figure 13 (continued)

(c) Vertical velocity in cm/sec.

(d) Fractional number density for O.

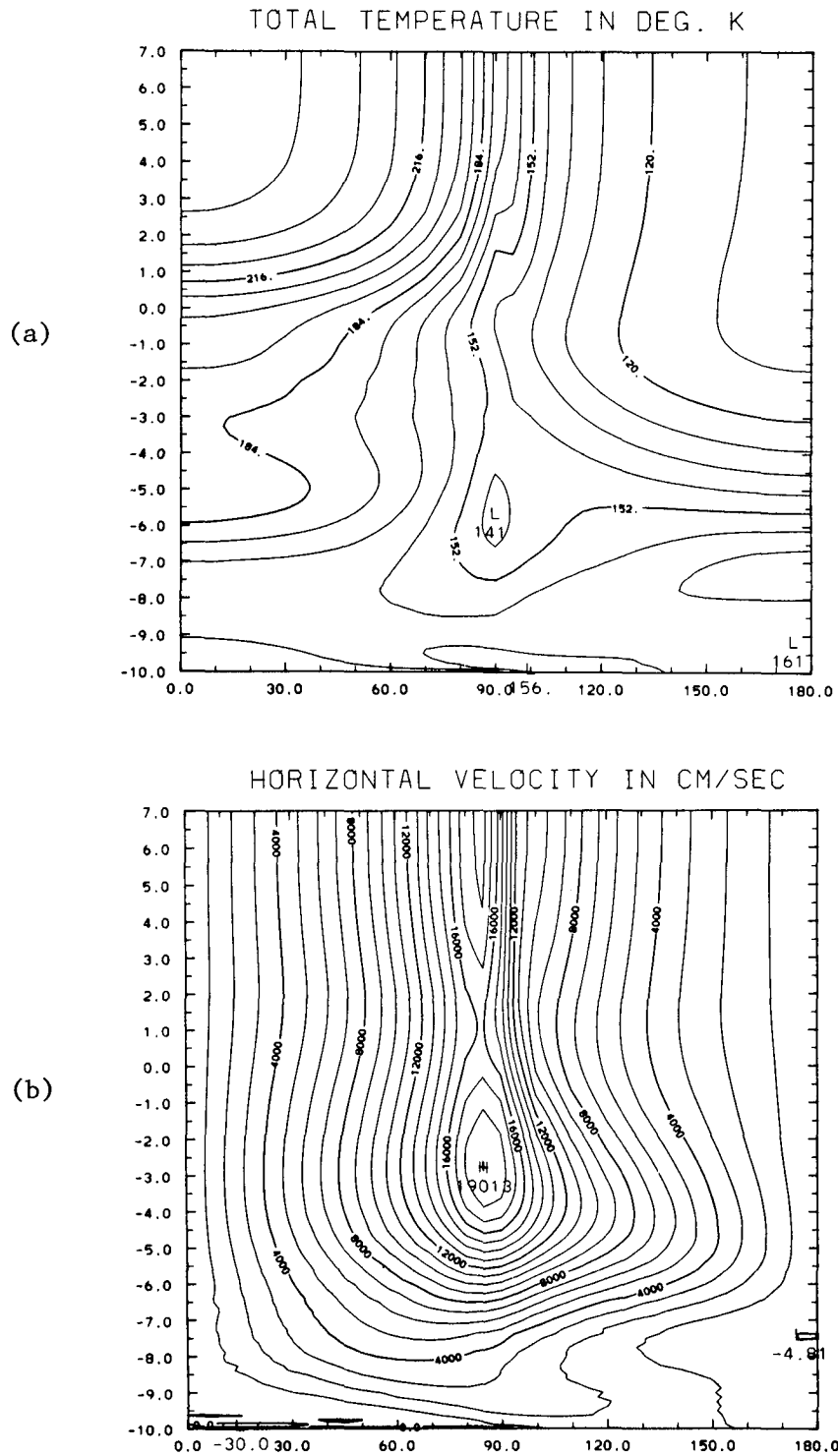


Figure 14. Solar minimum case contour plots (SZA vs Z):  
 (a) Total temperature in deg K.  
 (b) Horizontal velocity in cm/sec.



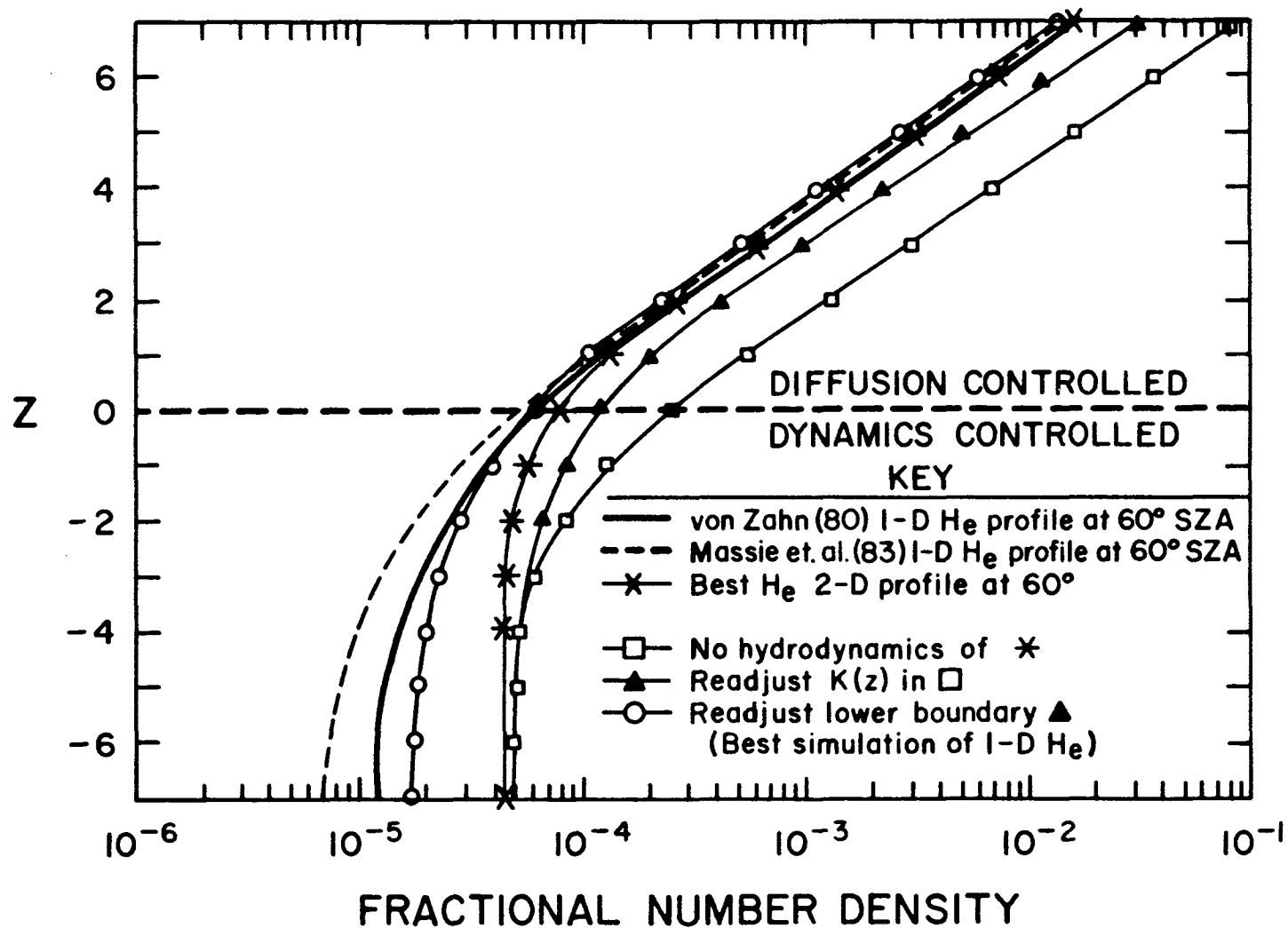


Figure 15. 60° SZA model helium (He) calculations. It is apparent from comparison of the one-dimensional and hydrodynamic model predictions for He at 100 km ( $Z \approx -8$ ) that the self-consistent large-scale dynamics is crucial to a proper calculation of composition. One-dimensional models are insufficient.

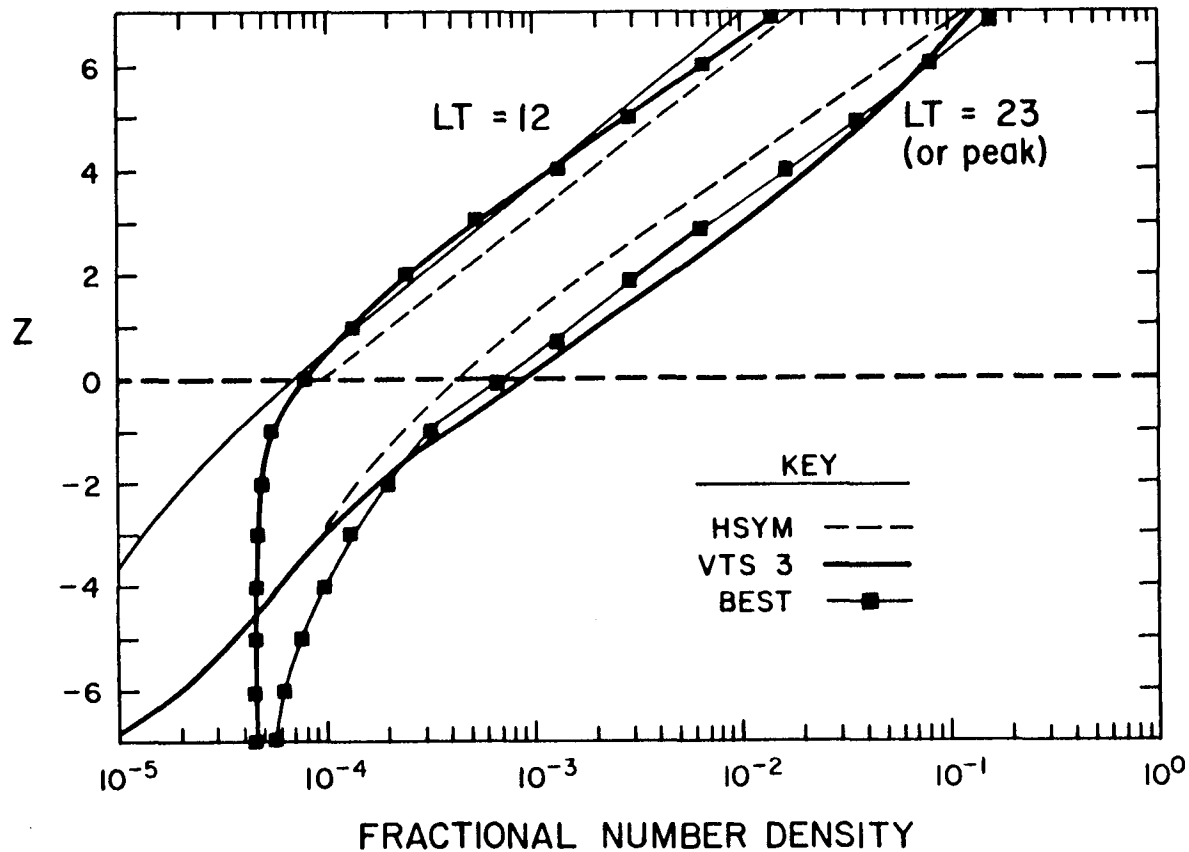


Figure 16. Venus two-dimensional model composition, helium: BEST EUV case. Noon and “nightside peak” profiles of helium are shown. The two-dimensional symmetric model approximately simulates dynamical conditions for the observed 3-4 AM helium peak near LT = 23.

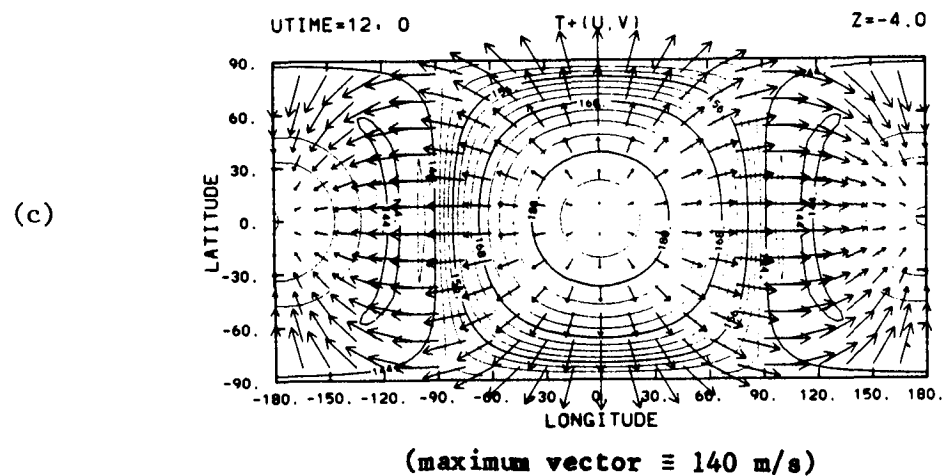
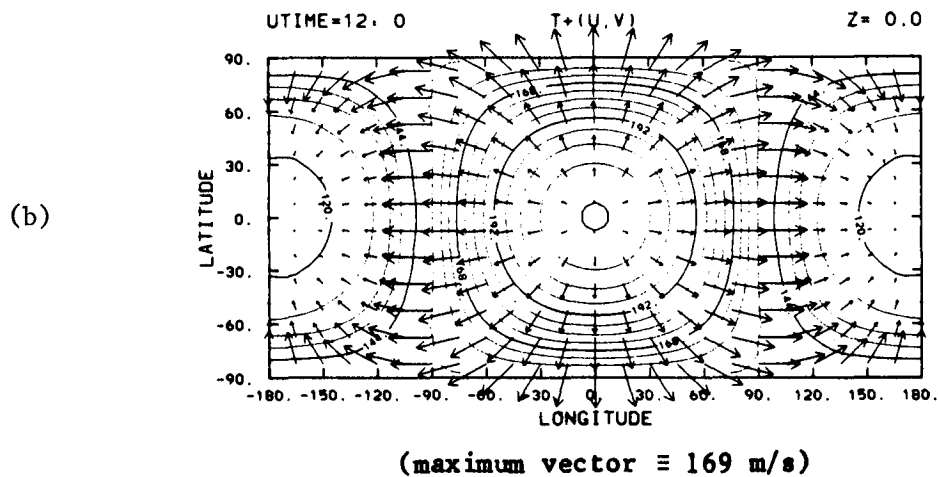
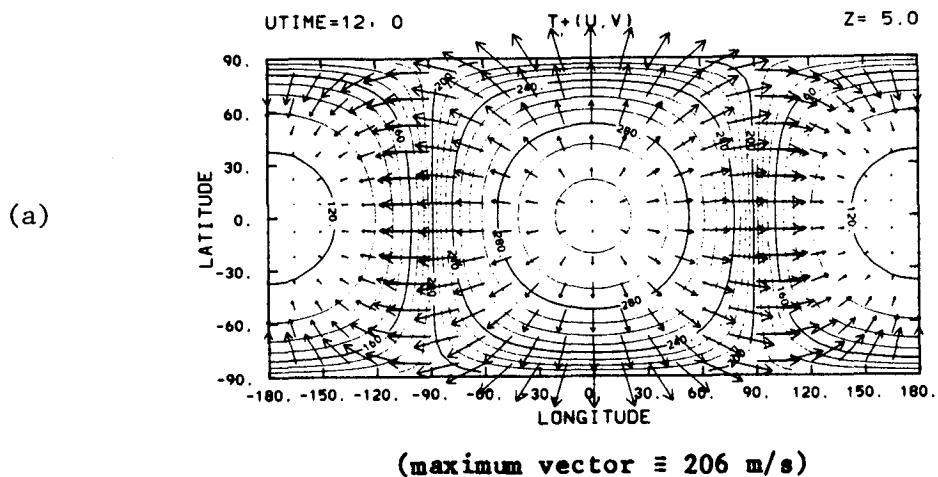


Figure 17.  $T + (u, v)$  contours on a pressure level slice for the Venus three-dimensional model adaptation of the terrestrial TGCM (a)  $Z = 5$ , (b)  $Z = 0$ , (c)  $Z = -4$ . Temperature contours are superimposed upon horizontal wind vectors.

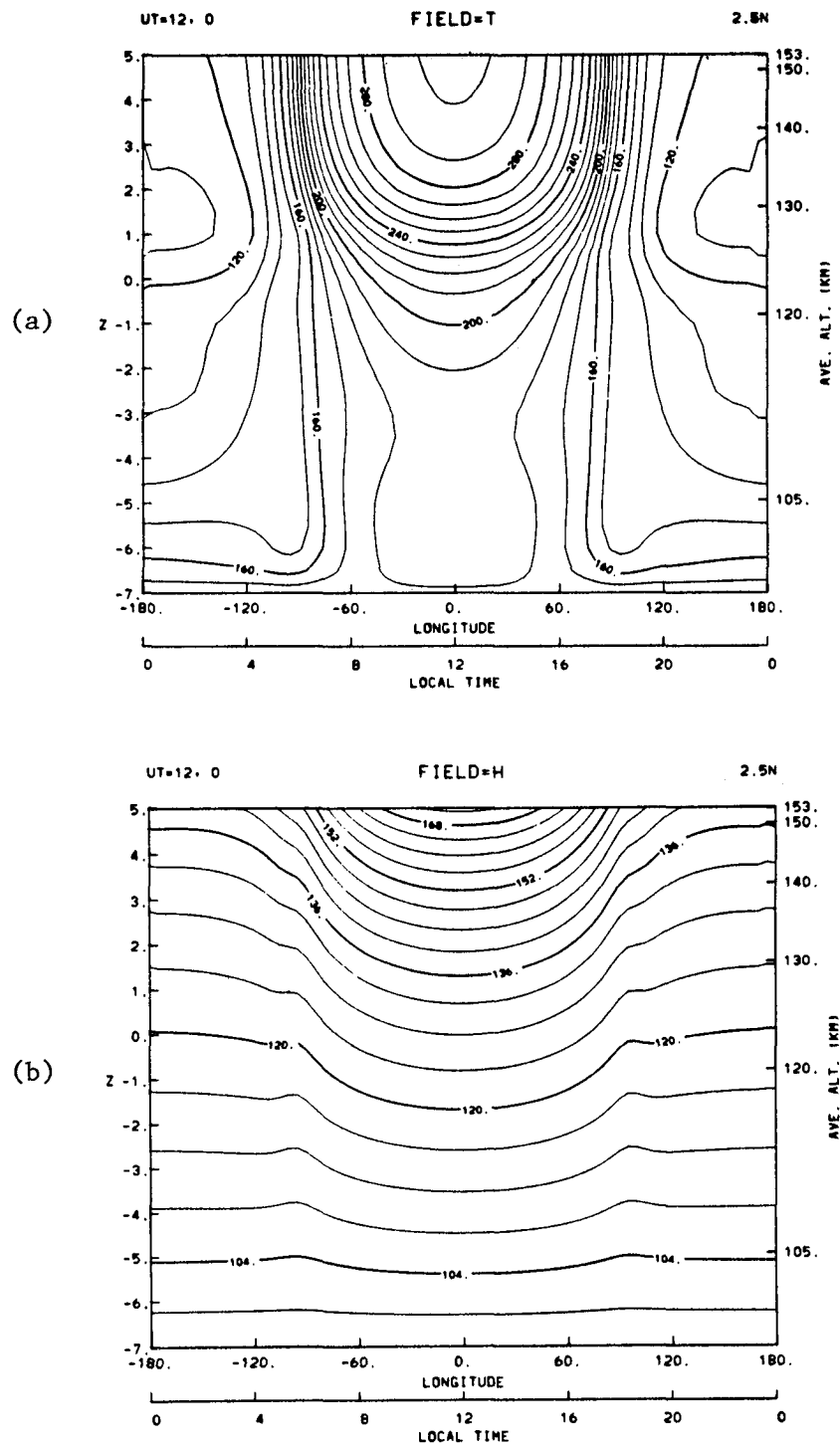


Figure 18. Equatorial slices (SZA vs Z) for the Venus three-dimensional adaptation of the terrestrial TGCM:

(a) T (total temperatures)

(b) h (height field in km)

